Title: Hydrogen Peroxide Solvates of 2,4,6,8,10,12-Hexanitro-2,4,6,8,10,12-Hexaazaisowurtzitane

Authors: Jonathan Caird Bennion; Nilanjana Chowdhury; Jeff W Kampf; Adam J. Matzger, Dr.

To be cited as: 10.1002/ange.201607130

Link to VoR: http://dx.doi.org/10.1002/ange.201607130

Hydrogen Peroxide Solvates of 2,4,6,8,10,12-Hexanitro-2,4,6,8,10,12-Hexaazaisowurtzitane

Jonathan C. Bennion, Nilanjana Chowdhury, Jeff W. Kampf and Adam J. Matzger*[a]

Abstract: Two polymorphic hydrogen peroxide (HP) solvates of 2,4,6,8,10,12-hexanitro-2,4,6,8,10,12-hexaazaisowurtzitane (CL-20) were obtained using the hydrated α-CL-20 as a guide. These novel HP solvates have high crystallographic densities (1.96 and 2.03 g/cm^3 respectively), high predicted detonation velocities/pressures (with one solvate possessing greater performance than that of ε-CL-20) and sensitivity similar to that of ε-CL-20. The use of hydrated materials as a guide will be important in the development of other energetic materials with hydrogen peroxide. These solvates represent an area of energetic materials that have yet to be explored.

The formation of hydrated materials is a common phenomenon throughout crystal engineering; in the field of pharmaceuticals it is estimated that at least a third of all pharmaceuticals are capable of forming hydrates.[1] In energetic materials the formation of various (hemi-, mono-, di-, etc.) hydrated materials is a problem that is also often encountered.[2] For example, the widely used energetics octahydro-1,3,5,7-tetranitro-1,3,5,7-tetrazocine (HMX) and 2,4,6,8,10,12-hexanitro-2,4,6,8,10,12-hexaazaisowurtzitane (CL-20) both form ¼ hydrates, γ-HMX and α-CL-20, which have inferior detonation properties compared to the respective high density forms, β-HMX and ε-CL-20. The detonation properties (velocity and pressure) are dependent on the density of a material (higher density translates to higher detonation velocity/pressure). While a hydrate may have a high density, hydration ultimately reduces the effective density of the energetic component(s) and as a result diminishes the performance of the material. Such an erosion of properties is similar to the case of cocrystals of energetic materials with non-energetic coformers.[3] This has been overcome through the use of other energetic molecules as coformers. Here we adapt this concept by using hydrogen peroxide as an energetic replacement for water of hydration in CL-20 thus improving the oxygen balance of the material.

Oxygen balance (OB) is the weight percent of oxygen released as a result of the complete conversion to neutral molecular components (CO_2, H_2O, N_2, etc.) upon detonation.[4] A positive OB denotes that there is excess oxygen in the system after full conversion, whereas a negative OB refers to an insufficient amount of oxygen and typically results in the generation of carbon soot and lower oxidized, toxic gases (CO, NO). The more negative the OB, the less gas that is generated from the detonation and as a result, the brisance or shattering effect of the material is diminished.[5] The vast majority of traditional energetic materials possess a negative OB with respect to CO_2: CL-20 (-11%), HMX (-22%) and 2,4,6-trinitrotoluene [TNT] (-74%). The inclusion of water molecules into the lattice of an energetic does not lead to increased OB because the oxygen atoms are already bonded to two hydrogens. However, the ability to incorporate water into the lattice suggested to us that a chemically similar, but more oxidizing solvent could improve rather than degrade performance. Hydrogen peroxide (HP) has seen extensive use as a propellant in both mono- and bi-propellant rockets.[6] HP has very low toxicity, minimal environmental impact compared to traditional perchlorate oxidizers and is also impact/shock insensitive in concentrated form.

In addition to the use of HP in rocket fuels, the peroxy group has seen some application into various energetic materials, such as triacetone triperoxide (TATP), diacetone diperoxide (DADP), hexamethylene triperoxide diamine (HMTD) and more recently into energetic materials containing peroxy acid and hydroperoxy groups.[7] The problem often encountered with these materials is that many are very sensitive to both thermal and impact initiation, while also possessing very poor OB due to the large amount of carbon contained within the backbones. Recently, DADP was shown to form a series of 1:1 cocrystals with 1,3,5-trichloro-2,4,6-trinitrobenzene (TCTNB), 1,3,5-tribromo-2,4,6-trinitrobenzene (TBTNB) and 1,3,5-triiodo-2,4,6-trinitrobenzene (TITNB) through interaction between the TXTNB (X = Cl, Br or I) coformer and the peroxy moiety.[8] These materials show feasibility for the formation of non-covalent interactions with the peroxy moiety. The substitution of HP for water of hydration might be predicted to form not only non-covalent interactions between the peroxy moieties, but also allow maintenance of the hydrogen bonding pattern.

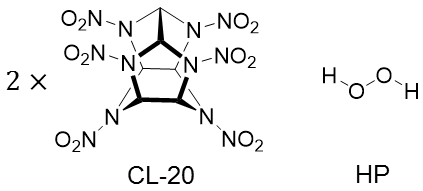

Figure 1. Chemical structures of the pure components for the CL-20 polymorphic solvates (**1** and **2**): CL-20 and HP.

The hydrated form of CL-20, α-CL-20, is generally regarded as a ¼ hydrate, but can also exist as a ½ hydrate.[2d] The unit cell of the ¼ hydrate contains a total of eight CL-20 molecules with sufficient void space to encompass two solvent molecules. The packing coefficient (C_k), a measure of the efficiency that molecules occupy the unit cell volume, can be determined by dividing the total molecular volume in a unit cell by the unit cell volume. By comparing the C_k of the high density ε-CL-20 (80.6%) to the lower density α-CL-20 (77.9%), it is evident that α-CL-20 possess void space that might be used to contain additional solvent molecules. Recently, it has been shown that water can be removed under heating/vacuum from α-

[a] J. C. Bennion, Dr. N. Chowdhury, Dr. J. W. Kampf, Prof. A. J. Matzger
Department of Chemistry and the Macromolecular and Engineering Program
University of Michigan
930 North University Avenue, Ann Arbor, MI 48109-1055 (USA)
E-mail: matzger@umich.edu

Supporting information for this article is given via a link at the end of the document. CCDC 1495519, 1495520 and 1495521 contain the supplementary crystallographic data for this paper. These data are provided free of charge by The Cambridge Crystallographic Data Centre.

CL-20 with little deformation of the lattice parameters.[9] This suggests the ability to utilize the void space for the formation of CL-20 solvates that will remain isostructural to the hydrated α-CL-20.

Disclosed here are two novel polymorphic solvates of CL-20 with HP, orthorhombic (**1**) and monoclinic (**2**); both materials form in a 2:1 molar ratio of CL-20 and HP (see Figure 1 for pure component structures). These represent the first examples of solvates with HP for any energetic material and may be influential for the further development of novel energetics.

The concomitant formation of **1** and **2** was initially observed from a 1:1 acetonitrile/HP (>90% H_2O_2) solution. Solvate **1** exhibits a rhombic habit, whereas **2** typically exhibits a polyhedron habit (Figure 3c and 4c respectively), and these crystals were separated and analyzed by powder X-ray diffraction. The powder pattern of **1** was indistinguishable from α-CL-20 (Supporting Information **S1** and **S2**), which suggests that the material is either simply α-CL-20 or an isostructural material with HP replacing the water molecules as hypothesized. Solvate **2**, on the other hand, is readily distinguishable from any of the other forms of CL-20 (Supporting Information **S3**).

The crystal structures of **1** and **2** were elucidated and determined to be 2:1 CL-20/HP solvates; crystallographic data are presented in Supporting Information Table S1 for α-CL-20, **1** and **2**. Both materials have high crystallographic densities: **1** has a density of 2.033 g/cm^3 at 295 K and **2** has a density of 1.966 g/cm^3 at 295 K. When compared to α-CL-20 (1.970 g/cm^3 at 295 K), the isostructural material **1** possesses a superior density and **2** possesses a density similar to that of the hydrated material. The OB for both **1** and **2** was determined to be -8.79%, an improvement with respect to both α-CL-20 (-10.84%) and pure CL-20 (-10.95%).

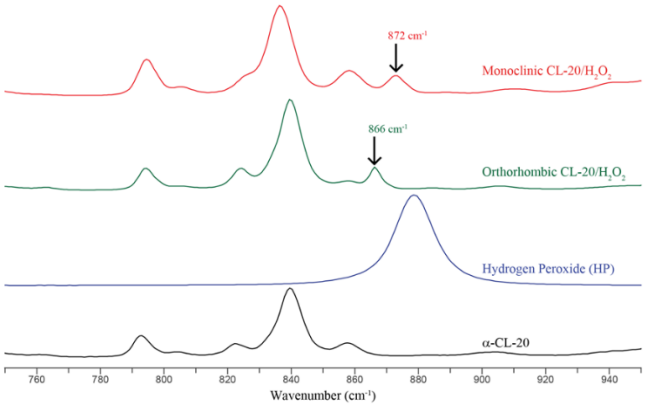

Figure 2. Raman spectra (700-1000 cm^{-1}) of α-CL-20, concentrated HP, **1** and **2**. Pure HP O-O peak is at 879 cm^{-1}.

One way of identifying the solvent content in a crystal structure is through the use of a PLATON/SQUEEZE calculation, which assesses the electron density contribution in the unit cell from the solvent.[10] Both the HP solvent present in the crystal structure of **1** and the H_2O in α-CL-20 (for these calculations the crystal structure of α-CL-20 was redetermined) sit on the same inversion center, leading to uncertainty into the existence of the HP in the material. The electron density was estimated to be 24 and 44 e$^-$/unit cell for α-CL-20 and **1**, respectively. The electron density for α-CL-20 corresponds roughly to the two water molecules present in the unit cell (10 e$^-$/molecule), whereas the higher electron density of 44 electrons for **1** corresponds to the presence of HP (18 e$^-$/molecule) in the isostructural material. The same routine was applied to **2** and the electron density was determined to be 79 e$^-$/unit cell, which corresponds closely to the four HP molecules in the 2:1 CL-20 solvate. The higher electron density suggests the presence of a novel material compared to α-CL-20, but given the tendency of SQUEEZE to overcount electron density, additional investigation via Raman spectroscopy and chemical analysis was carried out to further support these results.

The Raman spectra of both **1** and **2** were compared to all known forms of CL-20 and in particular to α-CL-20 (Figure 2 and Supporting Information **S4**). Both **1** and **2** resemble α-CL-20, with the exception of the addition/shifting of the O-O stretch present in the two new solvates. Pure HP has an O-O stretch at around 879 cm^{-1}, while the solvates have an O-O peak shifted to 866 and 872 cm^{-1} respectively for **1** and **2** (Figure 2). Additionally, shifting is present in the H-O stretch region for all three materials: α-CL-20 (3610 cm^{-1}), **1** (3557 cm^{-1}) and **2** (3517 cm^{-1}). The addition of the O-O peak and the shifting of the H-O peak in both **1** and **2** is indicative of an interaction between the CL-20 and HP. For both of the solvates, the higher population of electron density, along with the new and shifted peaks in the Raman spectra, confirms the existence of HP in these novel materials. The presence of the HP in the solvates was also quantified by a chemical test wherein the oxidation of triphenylphosphine with HP to triphenylphosphine oxide was measured by ^{31}P NMR and the proposed stoichiometry of 2 CL-20 to 1 HP was confirmed.

The formation of both CL-20 solvates rely on hydrogen bonding between the HP and the nitro groups of CL-20 as well as C-H hydrogen bonds between adjacent CL-20 molecules. The shortest interactions between the HP and CL-20 are highlighted (see Figures 3 and 4 respectively for solvates **1** and **2**). The HP in **1** hydrogen bonds with two CL-20 molecules and interacts with two nitro groups on each molecule in a bifurcated fashion, with intermolecular distances of 2.17/2.22 Å and 2.19/2.24 Å for each CL-20 molecule (Figure 3a). In contrast, the HP in solvate **2** hydrogen bonds with two CL-20 molecules, with an equivalent intermolecular distance of 2.25 Å. In both structures, the CL-20 molecules form linear chains through C-H and nitro hydrogen bonding with adjacent CL-20 molecules; these interactions are reminiscent to those seen in both 1:1 CL-20/TNT and 2:1 CL-20/HMX.[11] The shortest CL-20 C-H$\cdots$$NO_2$ interactions for **1** and **2** are 2.20 Å and 2.23/2.31 Å respectively. The same linear chain of CL-20 molecules in **1** is also seen in α-CL-20 (2.28 Å). Additionally in the structure of **2**, the repeat unit of two CL-20s with one HP (Figure 4a) forms a tape that extends through C-H hydrogen bonding between adjacent CL-20 molecules at 2.23 Å.

With the structural parameters obtained, the C_k values for these systems were determined for **1**, **2**, and the pure components ε-CL-20 and α-CL-20.[12] Both solvates **1** (80.6%) and **2** (78.1%) possess C_k's higher than that of the α-CL-20 (77.9%), whereas **1** equals the C_k of ε-CL-20 (80.6%). The

difference of the C_k between **1** and α-CL-20 is expected for two reasons: the increased ratio of CL-20/HP (2:1) compared to the CL-20/H_2O (4:1) and the increased size/volume of the HP compared to the H_2O molecules. The C_k of solvate **1** equals that of ε-CL-20 through the incorporation of additional oxidizer, while also possessing a density on par to that of ε-CL-20 (2.04 g/cm^3).

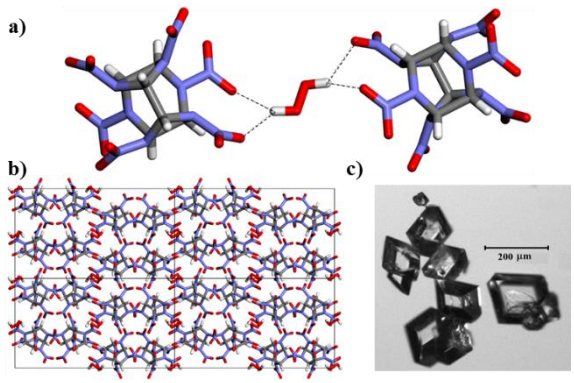

Figure 3. The 2:1 CL-20/HP orthorhombic solvate (**1**). a) Hydrogen bonding interaction between CL-20 and HP. b) Unit cell viewing down the *a*-axis. c) Typical rhombic habit morphology of the orthorhombic polymorph.

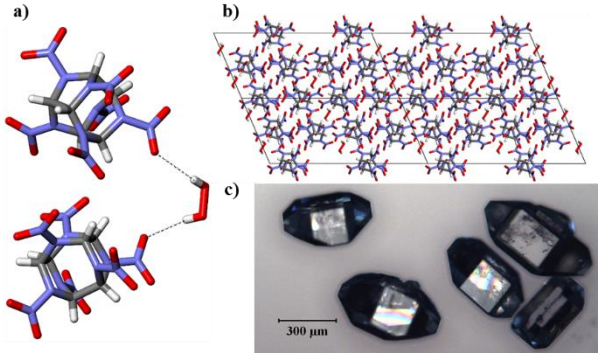

Figure 4. The 2:1 CL-20/HP monoclinic solvate (**2**). a) Hydrogen bonding interaction between CL-20 and HP. b) Unit cell viewing down the *a*-axis. c) Typical polyhedron habit morphology of the monoclinic polymorph.

The thermal properties of both **1** and **2** were determined via differential scanning calorimetry (DSC) and thermogravimetric analysis (TGA). The DSC traces show endothermic peaks at 165, 190 and 158 °C for **1**, **2** and α-CL-20 respectively, and decomposition around 250 °C for all three materials (Supporting Information **S9**). Raman spectroscopy and PXRD were performed after holding the temperature just past the respective endothermic peaks of **1** and **2**, and this thermal event was determined to correspond to the release of HP and subsequent conversion to γ-CL-20. The difference in the desolvation temperature of the two materials arises from the difference in both the hydrogen bonding between the two components and the packing arrangements of the CL-20 molecules in the unit cell; **1** possesses a channel for the HP to escape from, while the HP in **2** is contained in a cage of CL-20 molecules. The conversion of the solvates to γ-CL-20 explains why all three materials decompose at the same temperature. Furthermore, the TGA thermograms show the loss of HP at the corresponding endothermic peak temperatures (Supporting Information **S10** and **S11**). The thermal stability of these materials is an important performance criterion to consider in their future application as energetics.

The sensitivity of an energetic material to various external stimuli (impact, friction, electrostatic shock, etc.) must be determined before utility of a material can be fully realized. The sensitivity of **1** and **2** was determined via small-scale impact drop testing; for reference the Dh50 of ε-CL-20 and β-HMX are 29 and 55 cm, respectively (Supporting Information).[11b, 13] Solvate formation of CL-20 with HP results in material **1** possessing sensitivity (24 cm) just below that of ε-CL-20 (29 cm). Solvate **2** possesses sensitivity (28 cm) similar to that of ε-CL-20, yet with an increase to the overall OB of the system. These materials can be classified as sensitive secondary explosives. Currently CL-20 has seen some application in propellants, but with the need of oxidizers in the final formulation. Both **1** and **2** represent materials that, through solvate formation, are able to reduce/eliminate the need for the use of toxic oxidizers like perchlorates in the formulation of CL-20 propellants and should increase its potential utility.

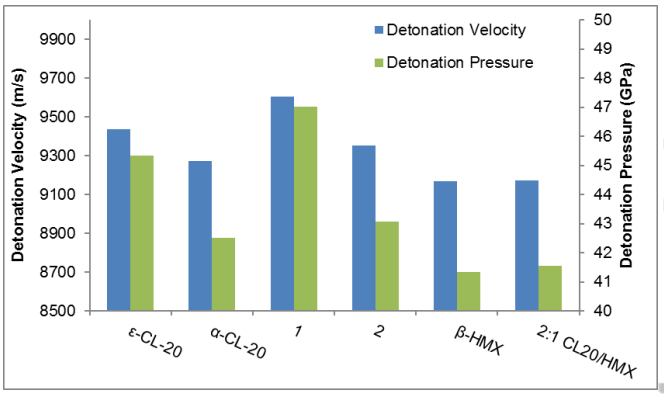

Figure 5. Detonation parameters (velocity and pressure) of ε-CL-20, α-CL-20, **1**, **2**, β-HMX and 2:1 CL-20/HMX are predicted with Cheetah 7.0 using the room-temperature (295 K) crystallographic densities of each material; detonation parameters for **1** at 2.033 g/cm^3 were calculated by extrapolating the detonation velocity vs. density and detonation pressure vs. density squared from the values determined at 99-90% of the crystallographic density given that the theoretical max density (%TMD) maxed out at only 2.013g/cm^3.

The detonation properties (velocity, pressure, etc.) were calculated using the thermochemical code Cheetah 7.0.[14] Cheetah calculations require both the chemical (molecular formula/density) and the thermodynamic (heat of formation) properties of a novel energetic material or formulation to predict the detonation velocity/pressure. The cocrystal/solvate performance properties are predicted by treating the materials as a formulation of the two components in their respective molar ratio. For the CL-20 solvates, the room temperature (295 K) densities for each material were used to predict both the detonation velocities and pressures as well as those properties for ε-CL-20, α-CL-20, β-HMX and the 2:1 CL-20/HMX cocrystal

(Figure 5). Both **1** (9606 m/s and 47.005 GPa) and **2** (9354 m/s and 43.078 GPa) have predicted detonation velocities and pressures that outperform α-CL-20, β-HMX and the 2:1 CL-20/HMX cocrystal. The orthorhombic solvate **1** is also projected to surpass the properties of ε-CL-20 (9436 m/s and 45.327 GPa), the gold standard for high performance energetic materials; this feat is accomplished through the incorporation of HP to increase the overall OB, with little degradation to the sensitivity of the materials.

In conclusion, we have discovered and characterized two polymorphic energetic solvates comprised of 2:1 molar ratios of the high explosive CL-20 and the oxidizer HP. The hydrated form of CL-20, α-CL-20, was used as a guide for the synthesis of the two HP solvates, and indeed one solvate remains isostructural to α-CL-20. These solvates represent the first example of hydrogen bonding interactions between HP and the nitro moiety, and the approach will be useful for the formation of additional HP solvated materials. Calculated detonation parameters (velocity and pressure) of the two solvates are predicted to surpass the performance of all known forms of HMX and all low density forms of CL-20, with the orthorhombic solvate **1** expected to exceed the properties of even ε-CL-20. The incorporation of HP into the crystal system allows for an easy and effective method for the improvement of the detonation properties, without the need for the development of new molecules. By utilizing existing hydrated energetic materials as a guide, the formation of additional isostructural HP solvates may be realized, which should possess superior performance to their pure energetic polymorphs.

Acknowledgements

This work was supported by the Army Research Office (ARO) in the form of a Multidisciplinary University Research Initiative (MURI) (grant number: W911NF-13-1-0387).

Keywords: solvates • hydrates • explosives • sensitivity • oxygen balance

[1] H. G. Brittain, *Polymorphism in Pharmaceutical Solids, Vol. 95*, Marcel Dekker, Inc., **1999**.

[2] a) E. V. Nikitina, G. L. Starova, O. V. Frank-Kamenetskaya, M. S. Pevzner, *Kristallografiya* **1982**, *27*, 485; b) R. Haiges, G. Belanger-Chabot, S. M. Kaplan, K. O. Christe, *Dalton Trans.* **2015**, *44*, 7586-7594; c) P. Main, R. E. Cobbledick, R. W. H. Small, *Acta Crystallogr. Sect. C* **1985**, *41*, 1351-1354; d) A. T. Nielsen, A. P. Chafin, S. L. Christian, D. W. Moore, M. P. Nadler, R. A. Nissan, D. J. Vanderah, R. D. Gilardi, C. F. George, J. L. Flippen-Anderson, *Tetrahedron* **1998**, *54*, 11793-11812; e) A. A. Dippold, T. M. Klapötke, *Chem. Eur. J.* **2012**, *18*, 16742-16753; f) H. Gao, J. n. M. Shreeve, *Chem. Rev.* **2011**, *111*, 7377-7436.

[3] a) K. B. Landenberger, A. J. Matzger, *Cryst. Growth Des.* **2010**, *10*, 5341-5347; b) K. B. Landenberger, A. J. Matzger, *Cryst. Growth Des.* **2012**, *12*, 3603-3609; c) D. I. A. Millar, H. E. Maynard-Casely, D. R. Allan, A. S. Cumming, A. R. Lennie, A. J. Mackay, I. D. H. Oswald, C. C. Tang, C. R. Pulham, *CrystEngComm* **2012**, *14*, 3742-3749.

[4] *The oxygen balance for an organic material can be calculated using the following equation: -1600(2a + 0.5b - d)/MW, where a, b, c, d are the number of carbon, hydrogen, nitrogen and oxygen atoms, respectively, and MW is the molecular weight of the material.*

[5] a) W. C. Lothrop, G. R. Handrick, *Chem. Rev.* **1949**, *44*, 419-445; b) A. Mustafa, A. A. Zahran, *J. Chem. Eng. Data* **1963**, *8*, 135-150.

[6] a) S. Bonifacio, G. Festa, A. R. Sorge, *J. Propul. Power* **2013**, *29*, 1130-1137; b) O. V. Romantsova, V. B. Ulybin, *Acta Astronaut.* **2015**, *109*, 231-234; cJ. J. Rusek, *J. Propul. Power* **1996**, *12*, 574-579.

[7] a) N.-D. H. Gamage, B. Stiasny, J. Stierstorfer, P. D. Martin, T. M. Klapotke, C. H. Winter, *Chem. Commun.* **2015**, *51*, 13298-13300; b) N.-D. H. Gamage, B. Stiasny, J. Stierstorfer, P. D. Martin, T. M. Klapötke, C. H. Winter, *Chem. Eur. J.* **2016**, *22*, 2582-2585; c) R. Matyáš, J. Pachman, *Propell., Explos. Pyrotech.* **2010**, *35*, 31-37; d) A. Wierzbicki, E. A. Salter, E. A. Cioffi, E. D. Stevens, *J. Phys. Chem. A* **2001**, *105*, 8763-8768.

[8] a) K. B. Landenberger, O. Bolton, A. J. Matzger, *Angew. Chem. Int. Ed.* **2013**, *52*, 6468-6471; b) K. B. Landenberger, O. Bolton, A. J. Matzger, *J. Am. Chem. Soc.* **2015**, *137*, 5074-5079.

[9] L. Pu, J.-J. Xu, X.-F. Liu, J. Sun, *J Energetic Mater.* **2016**, *34*, 205-215.

[10] A. L. Spek, *Acta Crystallogr. Sect. C* **2015**, *71*, 9-18.

[11] a) O. Bolton, A. J. Matzger, *Angew. Chem. Int. Ed.* **2011**, *50*, 8960-8963; b) O. Bolton, L. R. Simke, P. F. Pagoria, A. J. Matzger, *Cryst. Growth Des.* **2012**, *12*, 4311-4314.

[12] *Molecular volumes are calculated in Spartan14 V1.1.2 by determining the equilibrium geometry at the ground state for structures of the pure components with the semi-empirical AM1 method.*

[13] J. C. Bennion, A. McBain, S. F. Son, A. J. Matzger, *Cryst. Growth Des.* **2015**, *15*, 2545-2549.

[14] *Cheetah 7.0 calculations were preformed utilizing the Sandia JCZS product library revision 32.*

COMMUNICATION

Supercharged solvates: Two polymorphic hydrogen peroxide (HP) solvates of 2,4,6,8,10,12-hexanitro-2,4,6,8,10,12-hexaazaisowurtzitane (CL-20) were obtained with high crystallographic densities. Both solvates are predicted to have high detonation velocities/pressures (with the one solvate possessing greater performance than that of ε-CL-20). HP solvate formation allows for a simple method for improvements to the oxygen balance of existing materials.

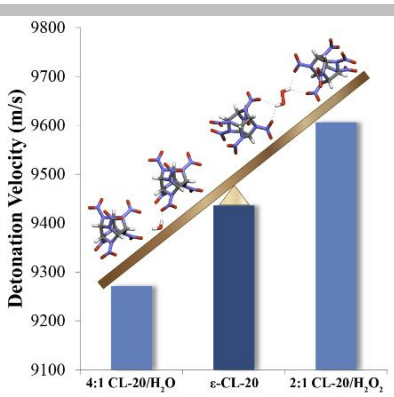

*Jonathan C. Bennion, Nilanjana Chowdhury, Jeff W. Kampf and Adam J. Matzger**

Page No. – Page No.

Hydrogen Peroxide Solvates of 2,4,6,8,10,12-Hexanitro-2,4,6,8,10,12-Hexaazaisowurtzitane

Hydrogen Peroxide Solvates of 2,4,6,8,10,12-Hexanitro-2,4,6,8,10,12-Hexaazaisowurtzitane

Jonathan C. Bennion[†], Nilanjana Chowdhury[†], Jeff W. Kampf[†] and Adam J. Matzger*[,†]

[†]Department of Chemistry and the Macromolecular Science and Engineering Program,

University of Michigan, 930 North University Avenue, Ann Arbor, Michigan 48109-1055,

United States

Table of Contents

SI 1. Experimental

Caution: *Although no unplanned detonations were encountered during this work, CL-20 is a dangerous high explosives and hydrogen peroxide is a strong oxidizing agent. Proper safety practices and equipment was used to prevent an explosion due to friction, heat, static shock, or impact. Be aware that the potential for severe injury exists if these materials are handled improperly.*

2,4,6,8,10,12-Hexanitro-2,4,6,8,10,12-hexaazaisowurtzitane (CL-20) was used as received from Picantinny Arsenal. The concentrated 98% hydrogen peroxide (HP) was used as received from PeroxyChem LLC.

Crystallization

Both polymorphic solvates of CL-20 (**1** and **2**) were initially obtained from 1:1 acetonitrile/HP solutions, with a small amount (~5 mg) of CL-20 dissolved, by slow evaporation and then conditions for their pure growth was determined. Similarly, the hydrated form of α-CL-20 was obtained by slow evaporation by dissolving a small amount (~5 mg) of CL-20 in a 1:1 acetonitrile/DI H_2O solution. The orthorhombic solvate could be scaled up easily through the slow addition of HP to the solution of CL-20. The monoclinic solvate could be scaled up conveniently with the use of solvent mediated transformation in a slurry of the pure components at room temperature, see below.

*2:1 CL-20/HP (**1**) monoclinic*

A 4 mL glass vial was loaded with 30 mg of ε-CL-20 (0.0685 mmol) which was dissolved in 300 µL of dry acetonitrile. To this was added 300 µL of concentrated H_2O_2 at which point the formation of thin plates of **1** was observed by optical microscopy. The vial was sealed/stirred gently for 15 minutes, before the crystal were collected. This solid was determined to be the 2:1 CL-20/HP orthorhombic solvate by both Raman spectroscopy and powder X-ray diffraction.

*2:1 CL-20/HP (**2**) monoclinic*

A 4 mL glass vial was loaded with 30 mg of ε-CL-20 (0.0685 mmol) which was dissolved in 200 µL of dry acetonitrile. To this was added 500 µL of concentrated H_2O_2 at which point a mixture

of orthorhombic and monoclinic solvates was obtained. The vial was sealed/stirred gently for 4 days, during which time the orthorhombic CL-20/HP crystals had disappeared and only the monoclinic CL-20/HP remained by optical microscopy. This solid was determined to be the 2:1 CL-20/HP monoclinic solvate by both Raman spectroscopy and powder X-ray diffraction.

Raman Spectroscopy

Raman spectra were collected using a Renishaw inVia Raman Microscope equipped with a Leica microscope, 633 nm laser, 1800 lines/mm grating, 50 μm slit and a RenCam CCD detector. Spectra were collected in extended scan mode with a range of 100-4000 cm^{-1} and then analyzed using the WiRE 3.4 software package (Renishaw). Calibration was performed using a silicon standard.

Powder X-ray Diffraction (PXRD)

Powder X-ray diffraction patterns were collected on a Bruker D8 Advance diffractometer using Cu-Kα radiation (λ = 1.54187 Å) and operating at 40 kV and 40 mA. Samples were prepared by finely grinding and packing into the depression of a glass slide. The powder patterns were collected by scanning 2θ from 5° to 50° with a step size of 0.02° and a step speed of 0.5 seconds. The data was processed using Jade 8 XRD Pattern Processing, Identification & Quantification analysis software (Materials Data, Inc.).[1] The powder patterns were all compared to their respective simulated powder patterns from the single crystal X-ray diffraction structures and were found to be in significant agreement with the predicted patterns.

Single Crystal Structure Determination

Single crystal X-ray diffraction data for **1**, **2** and α-CL-20 were collected using a Rigaku AFC10K Saturn 944+ CCD-based X-ray diffractometer equipped with a low temperature device and Micromax-007HF Cu-target micro-focus rotating anode (λ = 1.54187 Å) operated at 1.2 kW power (40 kV, 30 mA). The X-ray intensities were measured at 85(1) K with the detector placed at a distance 42.00 mm from the crystal. The data was processed with CrystalClear 2.0 (Rigaku)[2] and corrected for absorption. The structures were solved and refined with the Bruker SHELXTL (version 2008/4)[3] software package using direct methods. All non-hydrogen atoms were refined anisotropically with the hydrogen atoms placed in a combination of refined and idealized

positions. Funding for single crystal X-ray analysis was from NSF Grant CHE-0840456 for the Rigaku AFC10K Saturn 944+ CCD-based X-ray diffractometer.

CCDC 1495519, 1495520 and 1495521 contain the supplementary crystallographic data for this paper. These data are provided free of charge by The Cambridge Crystallographic Data Centre.

Table S1. Crystallographic Data for α-CL20 and CL-20 Solvates (Collected at 85 K)

Material	**α-CL-20**	**1**	**2**
Stoichiometry	4:1	2:1	2:1
Morphology	Plate	Rhombic	Polyhedron
Space Group	Pbca	Pbca	C2/c
a (Å)	9.4765(2)	9.4751(2)	28.4497(7)
b (Å)	13.1394(2)	13.1540(10)	8.9596(2)
c (Å)	23.3795(16)	23.4266(4)	12.7807(9)
α (°)	90	90	90
β (°)	90	90	113.397(8)
γ (°)	90	90	90
V0olume ($Å^3$)	2911.11	2919.79	2989.9
Z	8	8	8
ρ_{calc} (g/cm^3)	2.020	2.071	2.041
Data/Parameter	2669/287	2648/324	2696/312
R_1/wR_2	3.46/9.38	3.28/8.82	4.10/9.49
GOF	1.008	1.058	1.134

Differential Scanning Calorimetry (DSC)

Thermograms for each samples were recorded on a TA Instruments Q20 DSC equipped with a RCS90 chiller. All experiments were run in Tzero™ hermetic aluminum DSC pans under a nitrogen purge with a heating rate of 10 °C/min, while covering the temperature range of 40 °C to 300 °C. The instrument was calibrated using an indium standard. Thermograms were analyzed using TA Universal Analysis 2000, V 4.5A.

Thermogravimetric Analysis (TGA)

Thermograms for each samples were recorded on a TA Instruments Q50 TGA. All experiments were run in platinum TGA sample pans with a stainless steel mesh cover under a nitrogen purge of 50 mL/min with a heating rate of 10 °C/min, while covering the temperature range of 35 °C to 450 °C. The instrument was calibrated using the Curie points of alumel and nickel standards. Thermograms were analyzed using TA Universal Analysis 2000, V 4.5A.

Drop Weight Impact Sensitivity Analysis

For the analysis of the sensitivity to impact, approximately 2 mg (± 10%) of material for each sample is contained within nonhermetic DSC pans and then struck by a freefalling 5 lb drop weight. A reproducible Dh_{50}, height of the 50% probability of detonation, is obtained by utilizing the Bruceton Analysis (up-and-down method) with varying drop heights. For reference the Dh_{50} of ε-CL-20 and β-HMX are 29 and 55 cm, respectively.

SI 2. Powder X-ray Diffraction of CL-20 Solvates

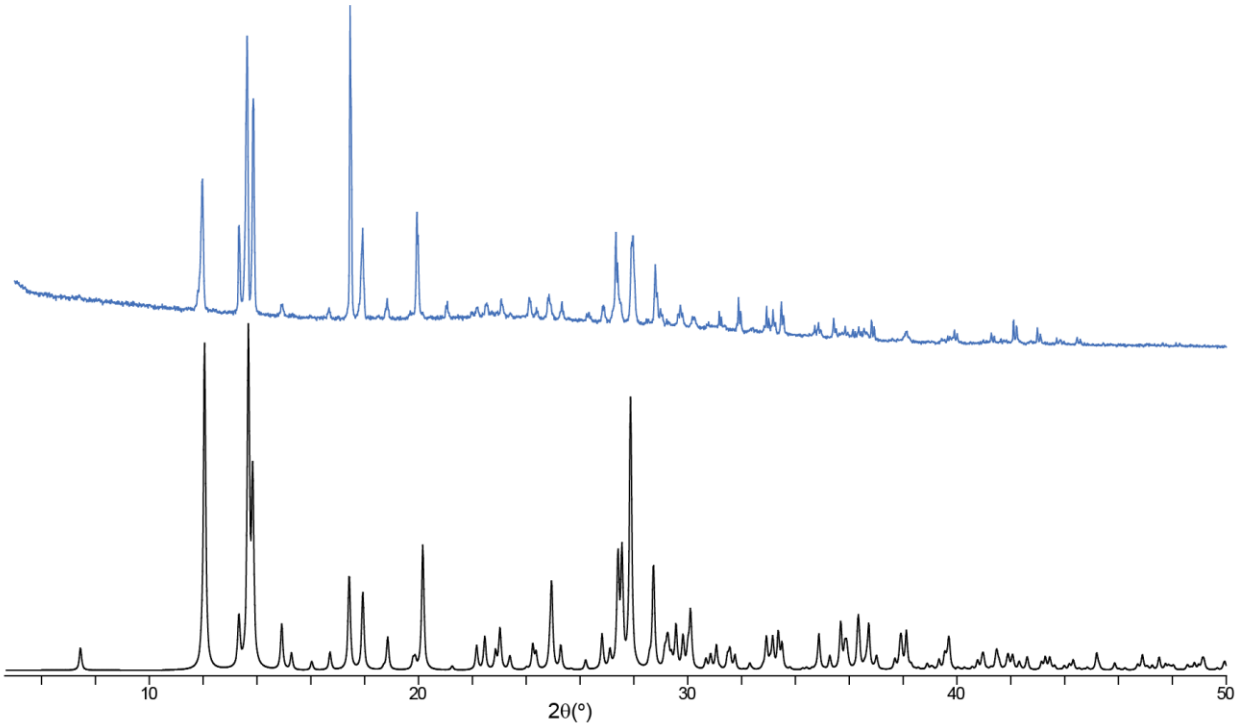

Figure S1. Powder patterns of **1** and the simulated structure of **α-CL-20** from the CIF (from top to bottom).

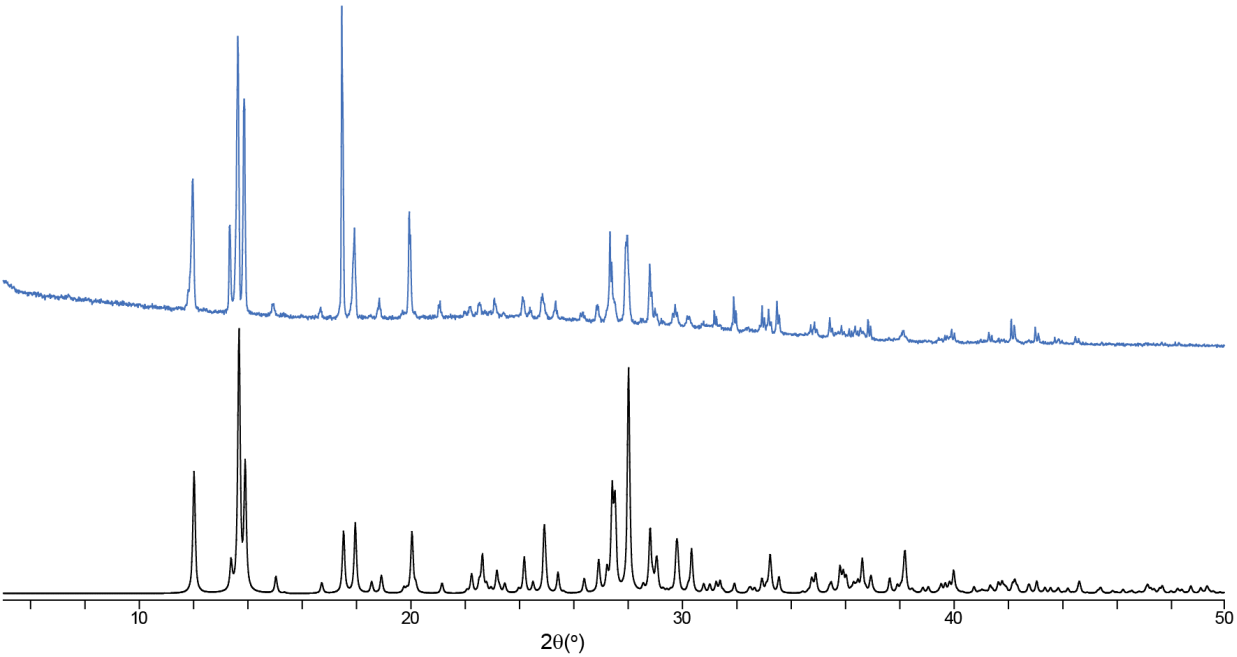

Figure S2. Powder patterns of **1** and the simulated structure of **1** from the CIF (from top to bottom).

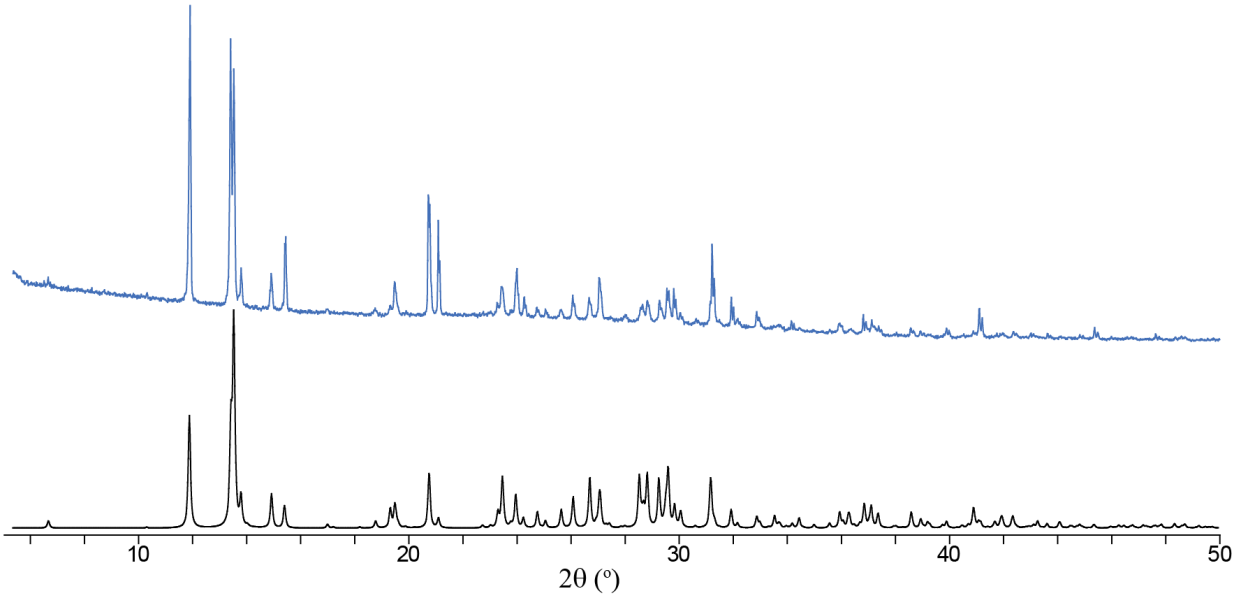

Figure S3. Powder patterns of **2** and the simulated structure of **2** from the CIF (from top to bottom).

SI 3. Raman Spectroscopy of CL-20 Solvates

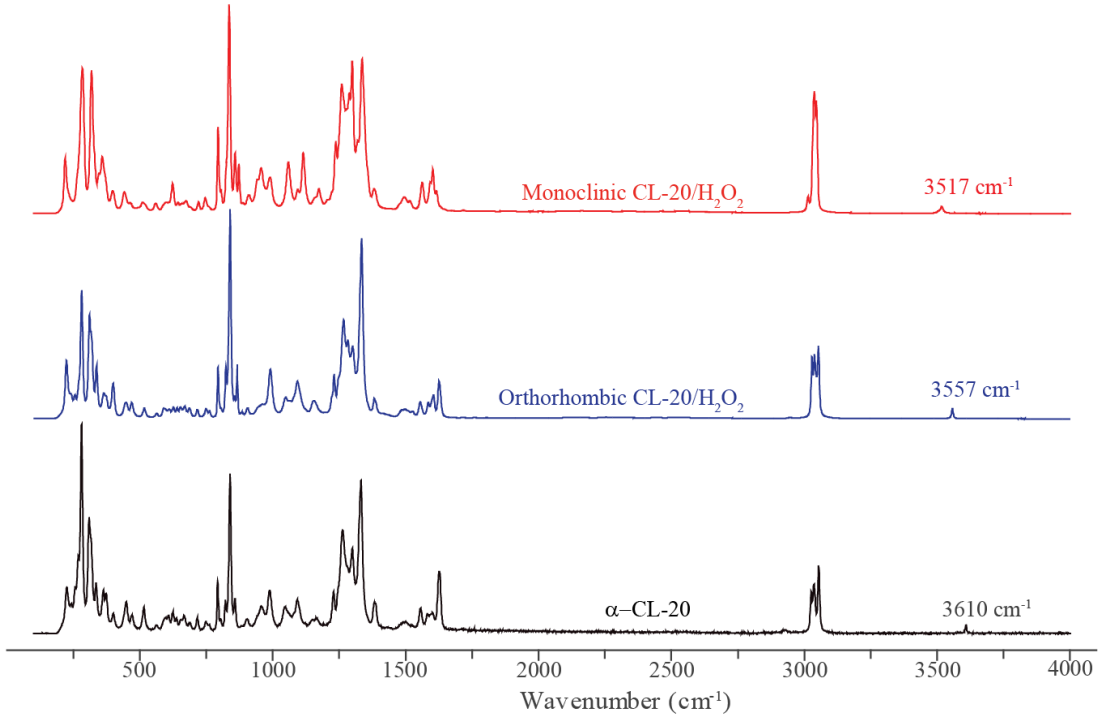

Figure S4. Full range (100-4000 cm^{-1}) Raman spectra of α-CL-20, **1** and **2** (from bottom to top).

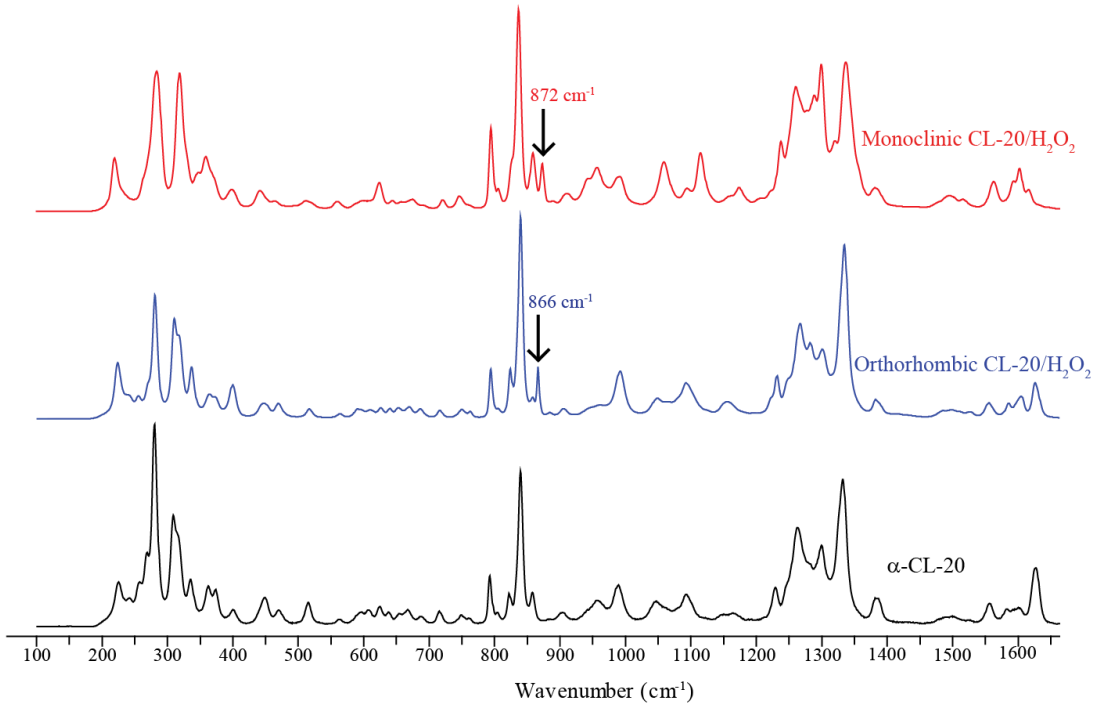

Figure S5. Zoomed in (100-1650 cm^{-1}) Raman spectra of α-CL-20, **1** and **2** (from bottom to top). Pure HP O-O peak is at 879 cm^{-1}.

SI 4. ORTEP Diagrams of CL-20 Solvates

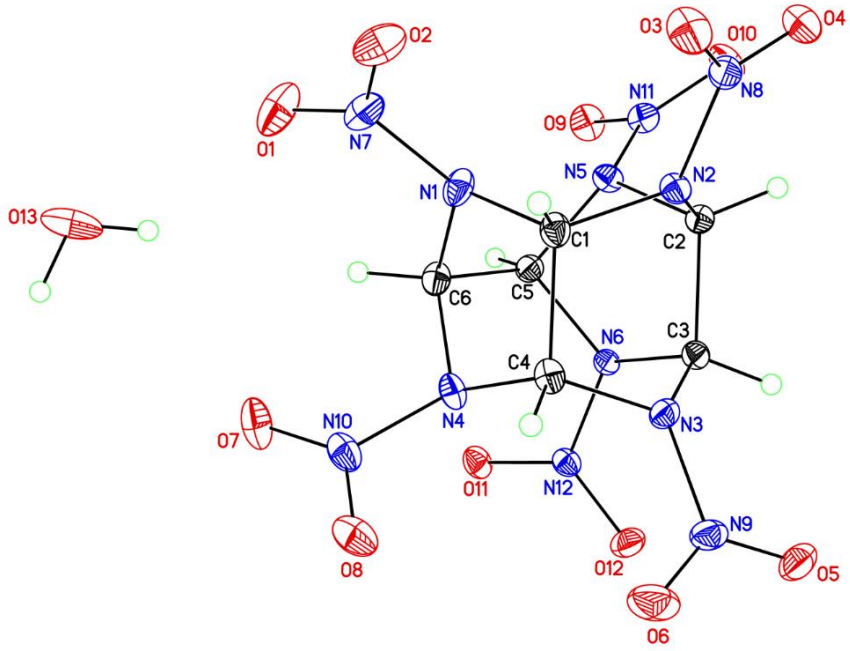

Figure S6. ORTEP diagram for **α-CL-20** collected at 85 K with thermal ellipsoids of 50% probability.

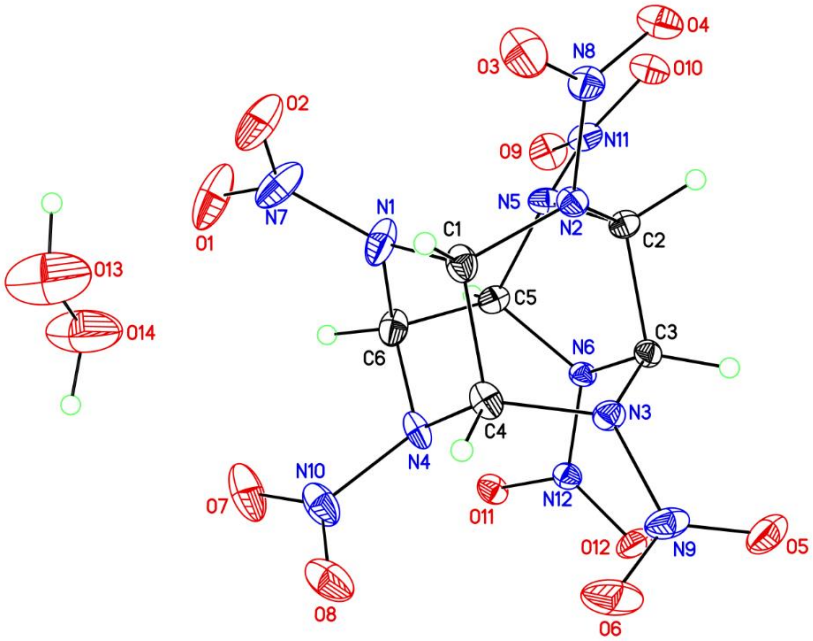

Figure S7. ORTEP diagram for **1**, orthorhombic, collected at 85 K with thermal ellipsoids of 50% probability.

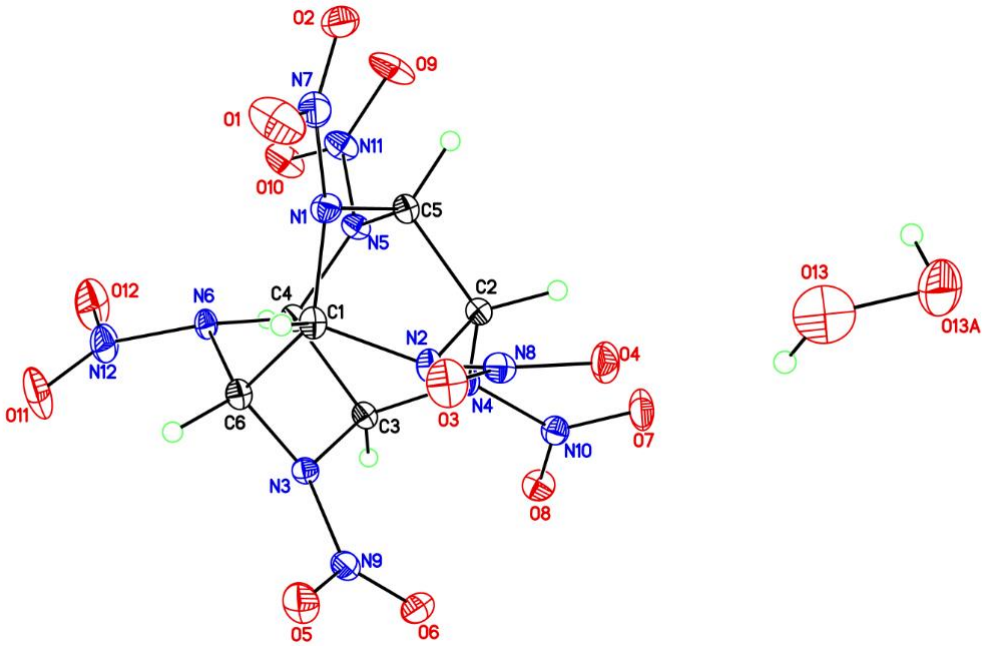

Figure S8. ORTEP diagram for **2**, monoclinic, collected at 85 K with thermal ellipsoids of 50% probability.

SI 5. Differential Scanning Calorimetry of CL-20 Solvates

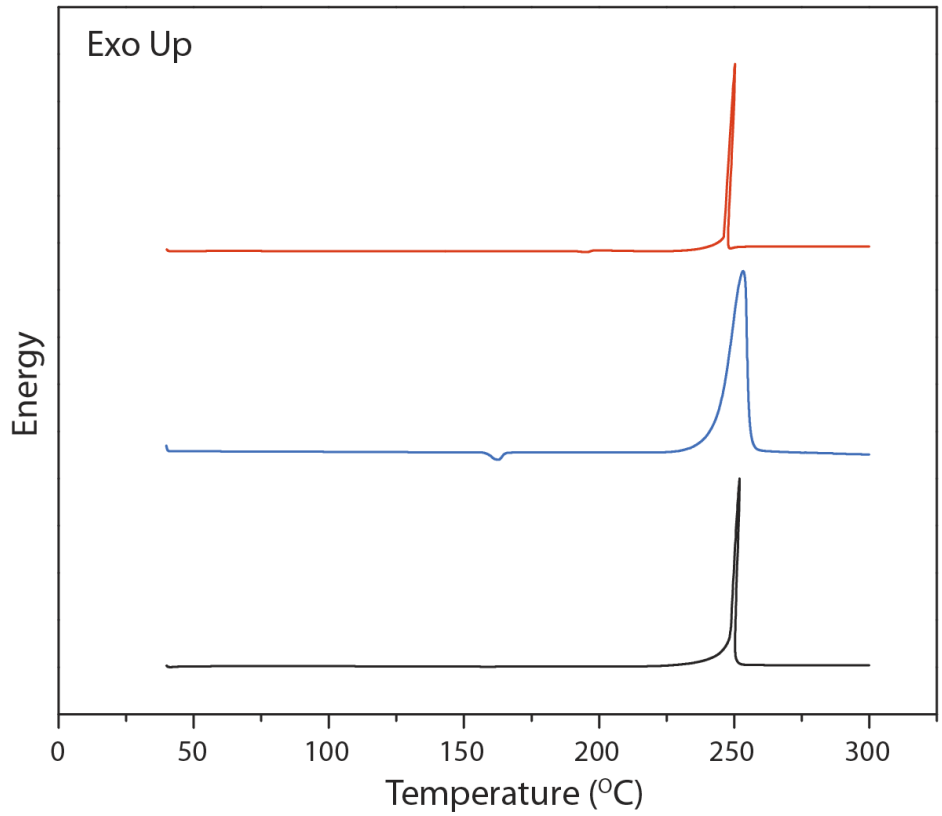

Figure S9. Typical DSC traces of α-CL20, **1** and **2** (from bottom to top).

SI 6. Thermogravimetric Analysis of CL-20 Solvates

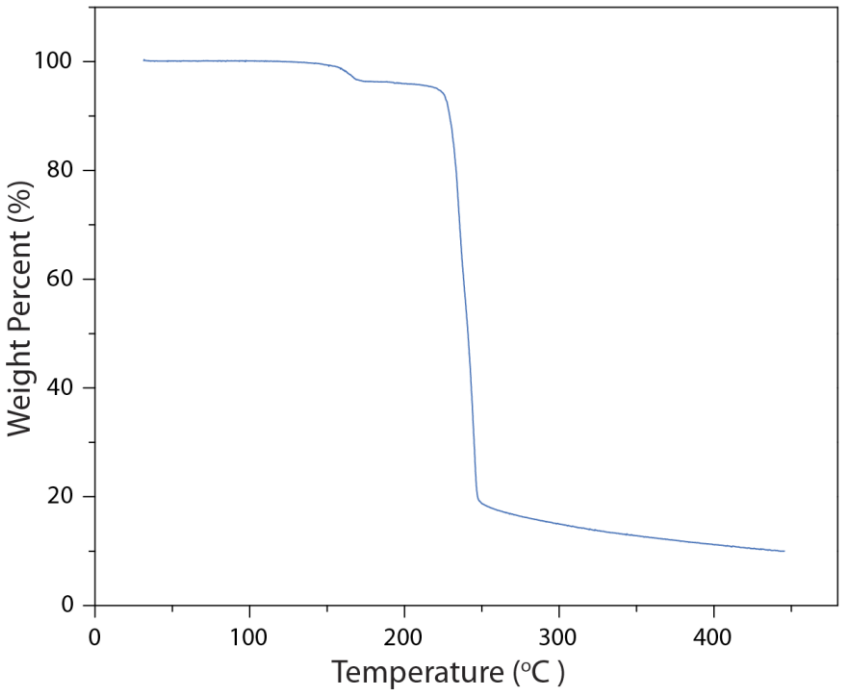

Figure S10. Typical TGA traces of **1**.

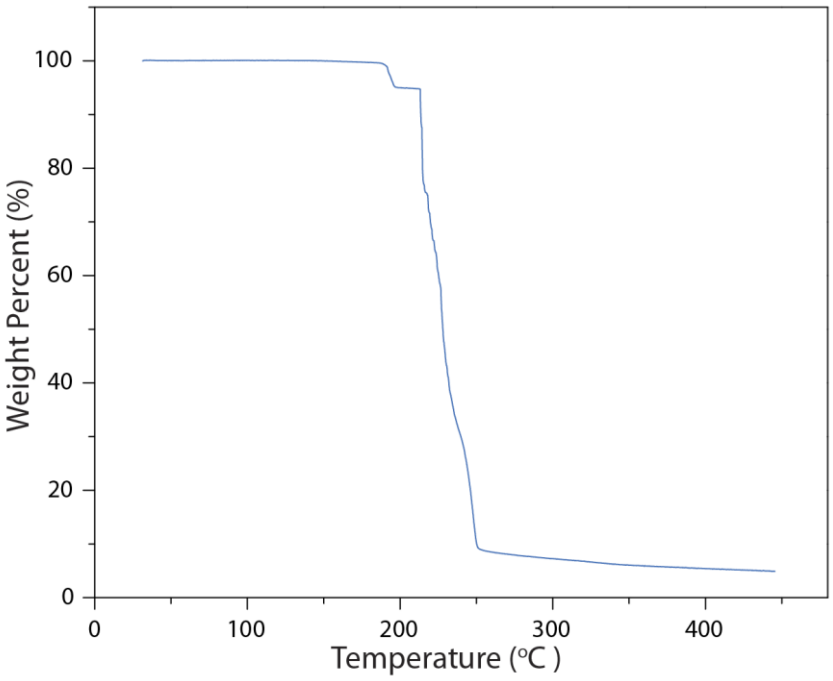

Figure S11. Typical TGA traces of **2**.

SI 7. Morphology of CL-20 Solvates

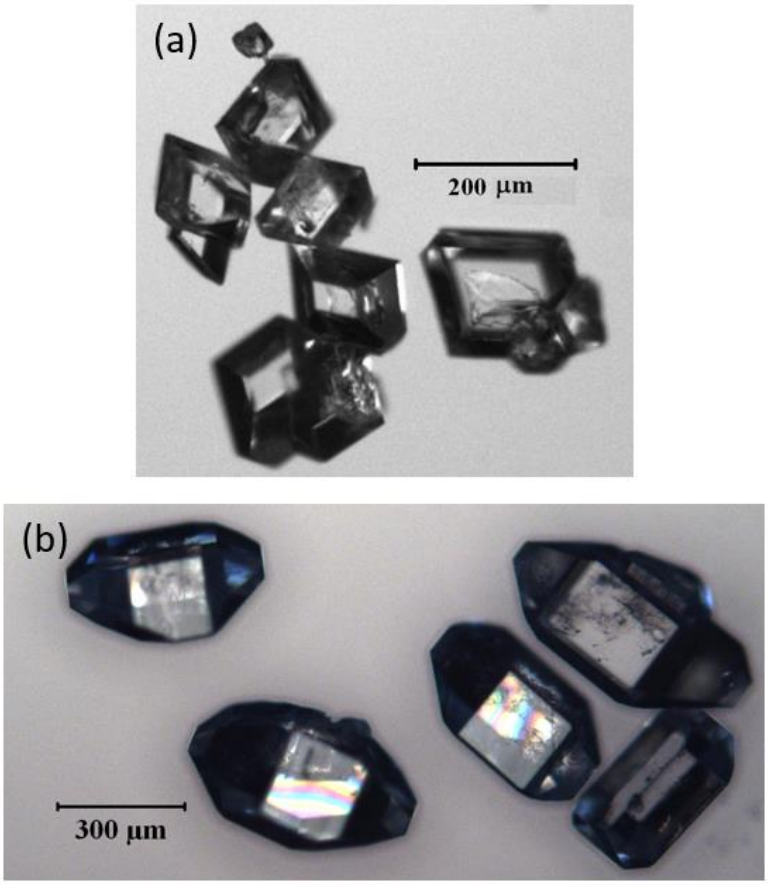

Figure S7. Typical habit morphology of the two polymorphs of the 2:1 CL-20/HP solvates (**1** and **2**): (a) orthorhombic; (b) monoclinic.

SI 8. References

(1) Jade Plus 8.2 ed.; Materials Data, Inc. 1995-2007.
(2) CrystalClear Expert 2.0 r12, Rigaku Americas and Rigaku Corporation (2011), Rigaku Americas, 9009, TX, USA 77381-5209, Rigaku Tokyo, 196-8666, Japan.
(3) Sheldrick, G.M. SHELXTL, v. 2008/4; Bruker Analytical X-ray, Madison, WI, 2008.